



Initial Placement for Fruchterman–Reingold Force Model with Coordinate Newton Direction

Hiroki Hamaguchi  Naoki Marumo  Akiko Takeda 

Abstract—Graph drawing is a fundamental task in information visualization, with the Fruchterman–Reingold (FR) force model being one of the most popular choices. We can interpret this visualization task as a continuous optimization problem, which can be solved using the FR algorithm, the original algorithm for this force model, or the L-BFGS algorithm, a quasi-Newton method. However, both algorithms suffer from twist problems and are computationally expensive per iteration, which makes achieving high-quality visualizations for large-scale graphs challenging.

In this research, we propose a new initial placement based on the stochastic coordinate descent to accelerate the optimization process. We first reformulate the problem as a discrete optimization problem using a hexagonal lattice and then iteratively update a randomly selected vertex along the coordinate Newton direction. We can use the FR or L-BFGS algorithms to obtain the final placement. We demonstrate the effectiveness of our proposed approach through experiments, highlighting the potential of coordinate descent methods for graph drawing tasks. Additionally, we suggest combining our method with other graph drawing techniques for further improvement. We also discuss the relationship between our proposed method and broader graph-related applications.

Index Terms—Graph Drawing, Optimization, Fruchterman–Reingold Algorithm, L-BFGS algorithm



1 INTRODUCTION

GRAPH is a mathematical structure representing pairwise relationships between objects, and graph drawing is a fundamental task in information visualization. Indeed, numerous kinds of models and algorithms have been proposed, and among these, one of the most popular choices is force-directed graph drawing.

In force-directed graph drawing, the force model is composed of particles with forces acting between them. The equilibrium of these forces is considered suitable for graph visualization, and algorithms aim to find this equilibrium state. Among the force models [6, 19], the Fruchterman–Reingold (FR) force model [8, 21] is the most prominent one, regarded as flexible, intuitive, and simple. It is widely used in various graph drawing libraries such as NetworkX [14], Graphviz [7], and igraph [4].

Contrary to the advantages above, the algorithms using this model face challenges in producing high-quality visualizations for large-scale graphs. The most critical issue is that *twist* slows down the force simulation. The term *twist* refers to unnecessary folded and tangled structures in the visualized graph [3, 31]. The results by the FR and L-BFGS algorithms from a random initial placement shown in Fig. 1 highlight these twist issues. Even if a graph has a simple structure, twists often occur, which cancel out the forces and lead to stagnation and suboptimal visualization outcomes. The FR algorithm is proposed alongside the force model and the most commonly used approach, but the results are excessively twisted. The L-BFGS algorithm, a family of quasi-Newton methods, has been reported as a more practical approach for graph drawing [17] and achieves better results than the FR algorithm. While this algorithm can partially address the twist problem, it sometimes requires many iterations. As shown in the figure, it may fail to

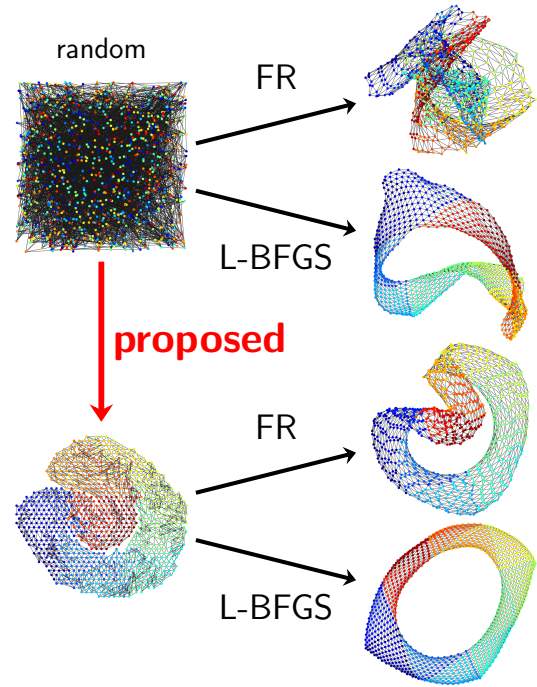


Fig. 1. Comparison of the algorithms for the `jagmesh1`.

achieve optimal visualization within a limited number of iterations. Furthermore, these algorithms suffer from high computational complexity when directly applied, $\mathcal{O}(|V|^2)$ per iteration, where $|V|$ is the number of vertices.

Another approach to the twist problem is pre-processing to find a better initial placement. A pre-processing step with Simulated Annealing (SA) is known to be effective [11] since SA can avoid getting stuck in local optima and leads to a

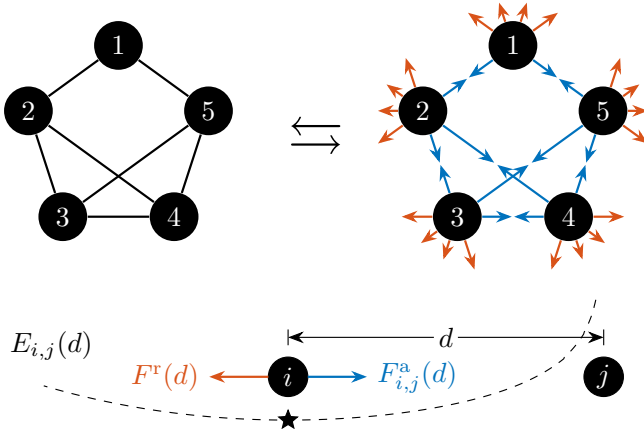


Fig. 2. (Top) The illustration of the force model. Forces act on every pair of vertices. (Bottom) Forces $F_{i,j}^a(d)$ and $F^r(d)$ work between vertices i and j . The equilibrium of them is achieved at $d = k/\sqrt[3]{w_{i,j}}$, which equals k when $w_{i,j} = 1$.

better visualization combined with the FR algorithm. This work focuses only on unweighted, simple-structured, and small-scale graphs, leaving significant room to improve the effectiveness and extend the applicability. Refer to Sec. 3.2 for more details.

In this paper, we propose a new initial placement for the FR force model as depicted in Fig. 1. We provide an initial placement with fewer twists than random placement within a short time, accelerating the subsequent optimization process. We can use both FR and L-BFGS algorithms to obtain the final placement. This work extends the applicability of the initial placement idea to larger-scale, weighted, and complicated structured graphs. To achieve this, we optimize the position of vertices one by one with the coordinate Newton direction, leveraging the inherent structure and the sparsity of graphs. We also demonstrate its effectiveness through various experiments.

The rest of this paper is organized as follows. Sec. 2 introduces the FR force model. Sec. 3 reviews the related works. Sec. 4 proposes our initial placement algorithm. Sec. 5 shows the experimental results. Sec. 6 provides the rationale of our proposed algorithm. Finally, Sec. 7 discusses and concludes the paper.

2 FRUCHTERMAN–REINGOLD FORCE MODEL

Fruchterman and Reingold [8] proposed the FR force model for graph drawing based on the physical analogy of the system of particles. Through the simulation of these forces, the FR algorithm seeks the equilibrium positions. In contrast to this ordinary approach, we minimize the energy, also known as the stress, to seek equilibrium. This section reviews the model and clarifies the problem we solve.

Let $G = (V, E)$ be a connected undirected graph with vertex set $V = \{1, \dots, n\}$ and edge set E . Each edge $\{i, j\} \in E$ has weight $w_{i,j} > 0$. For convenience, we set $w_{i,j} = 0$ for $\{i, j\} \notin E$.

The FR force model assumes forces between vertices. For vertices i and j with a distance $d > 0$ between them, an

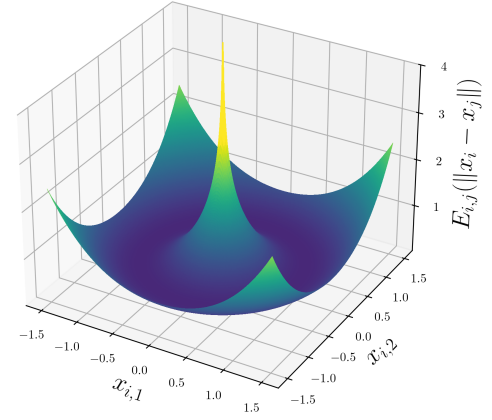


Fig. 3. Energy function $E_{i,j}(\|x_i - x_j\|)$ for $x_i = (x_{i,1}, x_{i,2})$, $x_j = (0, 0)$, $w_{i,j} = 1$, and $k = 1$.

attractive force $F_{i,j}^a(d)$ and a repulsive force $F^r(d)$ work as

$$F_{i,j}^a(d) := \frac{w_{i,j}d^2}{k}, \quad F^r(d) := -\frac{k^2}{d},$$

where $k > 0$ is a constant parameter, often set to $1/\sqrt{n}$. The scalar potential of these forces [17] is given by

$$\begin{aligned} E_{i,j}^a(d) &:= \int_0^d F_{i,j}^a(r) dr = \frac{w_{i,j}d^3}{3k}, \\ E^r(d) &:= \int_1^d F^r(r) dr = -k^2 \log d, \\ E_{i,j}(d) &:= E_{i,j}^a(d) + E^r(d). \end{aligned}$$

For simplicity, we define $E_{i,j}(0) = \infty$.¹ Let $\|\cdot\|$ denote the Euclidean norm in \mathbb{R}^2 . Then, the problem is to minimize the energy with $X := (x_1, \dots, x_n) \in \mathbb{R}^{2 \times n}$:

$$\underset{X \in \mathbb{R}^{2 \times n}}{\text{minimize}} \quad f(X) := \sum_{i < j} E_{i,j}(\|x_i - x_j\|). \quad (1)$$

The local minimum of f yields the equilibrium positions since $\nabla f(X)$ corresponds to the forces. Refer to Fig. 2 for the explanation of this force model.

As mentioned, we will only consider undirected connected graphs with non-negative weights. Although some algorithms can handle directed unconnected graphs with negative weights, we do not focus on such cases. For directed graphs, slight modifications of algorithms or converting graphs to undirected ones can be effective. For unconnected graphs, algorithms can be applied to each connected component independently. When negative weights are present, the optimization problem (1) can be unbounded, but with non-negative weights and the connectivity of G , the problem is always bounded and solvable.

While the energy function $E_{i,j}$ is convex and minimized when $d = k/\sqrt[3]{w_{i,j}}$, a function $x_i \mapsto E_{i,j}(\|x_i - x_j\|)$ is non-convex for a fixed x_j . Additionally, $E_{i,j}$ is not Lipschitz continuous as it diverges when $d \rightarrow 0$. These properties highlight the difficulty of the problem. Refer to Fig. 3 for an illustration of $E_{i,j}$.

1. Or, we can use $-k^2 \log(d + \epsilon^r)$ for $E^r(d)$ to prevent divergence, where ϵ^r is a small constant.

3 RELATED WORKS

We briefly introduce some critical related works.

3.1 Algorithms for FR Force Model

As mentioned in Sec. 1, we can use the FR and L-BFGS algorithms to visualize graphs with the FR force model. These algorithms solve the problem (1), and both can be combined with the initial placement we will propose in Sec. 4. For further details on the algorithms, see Sec. 8.

3.2 Pre-Processing by Simulated Annealing

Let $Q^{\text{circle}} := \{(\cos(2\pi i/n), \sin(2\pi i/n)) \mid 1 \leq i \leq n\}$ be the points on a unit circle in \mathbb{R}^2 . For an unweighted graph G , let E_2 be a set of vertex pairs with a shortest path distance equal to 2. Let $\angle(a, b)$ denote the angle between the lines from the origin to the points a and b , measured in the interval $(-\pi, \pi]$. Ref. [11] defines the problem for the pre-processing of graph drawing as follows (with modified notations for consistency):

$$\begin{aligned} & \text{minimize} && \sum_{\{i,j\} \in E \cup E_2} |\angle(x_i, x_j)|, \\ & \text{subject to} && x_i \in Q^{\text{circle}} \quad \text{for } 1 \leq i \leq n, \\ & && x_i \neq x_j \quad \text{for } 1 \leq i < j \leq n. \end{aligned} \quad (2)$$

The problem (2) is a discrete optimization problem where the placement is limited to Q^{circle} and uses angles, not the function f . This study obtains a faster and better visualization by setting the result of Simulated Annealing (SA) for the problem (2) as an initial placement for the FR algorithm.

Still, the following limitations remain:

- The target graphs are restricted to unweighted ones.
- The layout is confined to a simple circle, which could be ineffective for complex structured graphs.
- The neighborhood in the SA is the random swapping of two vertices, making the optimization process inefficient for large-scale graphs.
- $|E_2|$ could be $\Theta(|V|^2)$, unable to leverage the sparsity of graphs if it exists.

We are dealing with these limitations and can regard our study as an extension of this prior work.

3.3 Graph Drawing by Stochastic Gradient Descent

When we study the graph drawing as an optimization problem, Stochastic Gradient Descent (SGD) for Kamada–Kawai (KK) layout [19] is one of the most notable works [33]. In the KK layout, we regard G as a complete graph and assign the energy function $E_{i,j}^{\text{KK}}$ to all edges. SGD in this context means to repeat randomly selecting an edge $\{i, j\}$ and updating x_i and x_j with the gradient of $E_{i,j}^{\text{KK}}$. In general, SGD is effective for solving various optimization problems.

Although applying SGD to the FR force model problem (1) is straightforward, it is ineffective for this problem. This is because the force model we consider assigns the same function $E_{i,j}(d) = -k^2 \log d$ to all $\{i, j\}$ such that $w_{i,j} = 0$. Optimizing $E_{i,j}$ only increases the distance between vertices i and j , no matter how close they are to each other in the optimal solution. Thus, the gradient of $E_{i,j}$ is not informative enough to find the optimal solution,

and we need to develop a new optimization method for the problem (1).

Still, the idea of randomly selecting an edge and updating its position is quite suggestive. Based on this idea, we propose to randomly select a vertex and update its position.

3.4 Newton Direction and Coordinate Newton Direction

Let us consider a strictly convex function $g: \mathbb{R}^n \rightarrow \mathbb{R}$ at x_0 . The Newton direction $d = -\nabla^2 g(x_0)^{-1} \nabla g(x_0)$ is an optimal direction for the second order approximation of g :

$$g(x_0) + \nabla g(x_0)^\top (x - x_0) + \frac{1}{2} (x - x_0)^\top \nabla^2 g(x_0) (x - x_0).$$

$x = x_0 + d$ is the minimizer of this approximation. Note that the Hessian matrix $\nabla^2 g(x_0)$ is positive definite since g is strictly convex. Although the Newton direction is essential in various iterative methods, it requires the computation of the inverse Hessian $\nabla^2 g(x_0)^{-1} \in \mathbb{R}^{n \times n}$, posing a high computational cost for large-scale problems.

Still, we can leverage the concept of the Newton direction in a different manner, the coordinate Newton direction. Instead of computing the inverse Hessian $\nabla^2 g(x_0)^{-1}$ in the entire variable space \mathbb{R}^n , we restrict the variable x to its coordinate block x_i with fewer dimensions, and compute $\nabla^2 g_i(x_i)^{-1} \nabla g_i(x_i)$ where g_i is a restricted function of g to x_i . Since the coordinate Newton direction computation is much cheaper than that of the Newton direction, we can repeat this procedure many times. In general, this idea is known as stochastic coordinate descent [29] or Randomized Subspace Newton (RSN) [12] in a broader context.

In particular, this coordinate Newton direction has an apparent natural affinity to the problem (1) in Sec. 2. We can compute the coordinate Newton direction by taking the position x_i of the vertex i as the coordinate block. Although directly applying this idea to the problem (1) is challenging, as we will discuss in Sec. 6, we leverage this coordinate Newton direction to propose our algorithm.

4 PROPOSED ALGORITHM

This section proposes a new initial placement algorithm for the problem (1), Algorithm 1. The algorithm solves a discrete optimization problem with stochastic coordinate descent to find an initial placement with fewer twists. Note that the proposed algorithm does not produce the final placement to the problem (1); the algorithm only provides an initial placement for the FR or L-BFGS algorithms.

4.1 Discrete Optimization Problem for Initial Placement

Even at the expense of accuracy, obtaining an approximate solution quickly is crucial for the initial placement. To obtain it, we simplify the problem (1) into a more manageable and well-behaved discrete optimization problem:

$$\begin{aligned} & \text{minimize} && f^a(X) := \sum_{\{i,j\} \in E} \frac{w_{i,j} \|x_i - x_j\|^3}{3k}, \\ & \text{subject to} && x_i \in Q^{\text{hex}} \quad \text{for } 1 \leq i \leq n, \\ & && x_i \neq x_j \quad \text{for } 1 \leq i < j \leq n, \end{aligned} \quad (3)$$

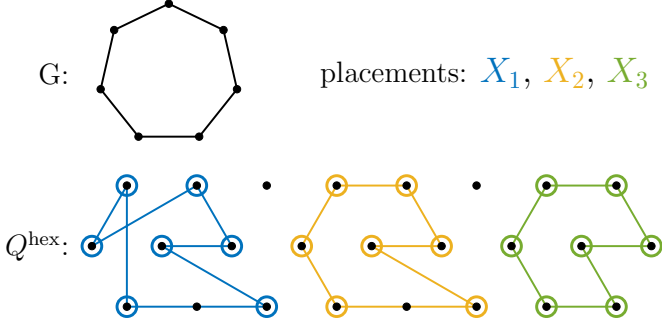


Fig. 4. Concept of Q . The assignment from V to a discrete point placement Q , especially a hexagonal lattice Q^{hex} . Apparently, among X_1, X_2, X_3 , the right one X_3 is the best placement for the problem (3).

where

$$Q^{\text{hex}} := \left\{ \left(q + \frac{1}{2}r, \frac{\sqrt{3}}{2}r \right) \mid q \in \mathbb{Z}, r \in \mathbb{Z} \right\}. \quad (4)$$

This section explains how this simplification is derived.

First, the problem (1) is equivalent to the following:

$$\text{minimize}_{X \in \mathbb{R}^{2 \times n}} \sum_{\{i,j\} \in E} \frac{w_{i,j} \|x_i - x_j\|^3}{3k} - \sum_{i < j} k^2 \log \|x_i - x_j\|.$$

This formulation separates the $\mathcal{O}(|E|)$ terms from $E_{i,j}^a$ and the $\mathcal{O}(|V|^2)$ terms from E^r .

Here, following previous research mentioned in Sec. 3.2, we fix the possible positions x_i of each vertex i to a discrete set of points Q , where $|Q| \geq |V|$. It means that we consider the following:

$$\begin{aligned} & \text{minimize}_{X \in \mathbb{R}^{2 \times n}} \sum_{\{i,j\} \in E} \frac{w_{i,j} \|x_i - x_j\|^3}{3k} - \sum_{i < j} k^2 \log \|x_i - x_j\|, \\ & \text{subject to } x_i \in Q \quad \text{for } 1 \leq i \leq n, \\ & \quad \quad \quad x_i \neq x_j \quad \text{for } 1 \leq i < j \leq n. \end{aligned}$$

The goal is to simplify the objective function and choose Q appropriately to derive a well-simplified problem.

Due to the sparsity of many practical graphs, $|E| \ll |V|^2$ holds. To leverage this sparsity for simplification, we want to drop the second term that arises from the repulsive energy E^r :

$$- \sum_{i < j} k^2 \log \|x_i - x_j\|.$$

We impose a condition on Q such that $\|q_i - q_j\| \geq \epsilon$ for all $q_i, q_j \in Q$ with $q_i \neq q_j$. In this case, the term above is negligible. Since $E^r(d) = -k^2 \log d$ is a convex function such that it decreases monotonically concerning d , for sufficiently large d , the value of $-k^2 \log d$ does not vary excessively. For too small d , we can prevent the divergence of the energy function by setting ϵ . Thus, under this condition, we drop the second term and derive the problem as:

$$\begin{aligned} & \text{minimize}_{X \in \mathbb{R}^{2 \times n}} \sum_{\{i,j\} \in E} \frac{w_{i,j} \|x_i - x_j\|^3}{3k}, \\ & \text{subject to } x_i \in Q \quad \text{for } 1 \leq i \leq n, \\ & \quad \quad \quad x_i \neq x_j \quad \text{for } 1 \leq i < j \leq n. \end{aligned}$$

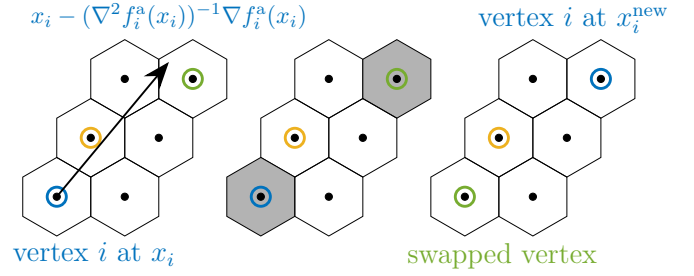


Fig. 5. One iteration of the proposed algorithm. Step1. Compute the coordinate Newton direction (blue). Step2. Decide x_i^{new} by rounding the direction and adding a random vector. Step3. Move the vertex and swap the vertices if there is a collision (swap blue and green vertices).

This means that we skip to consider the $\mathcal{O}(|V|^2)$ pairs (all pairs of $\{i, j\}$ with $1 \leq i < j \leq n$) by fixing the possible point placement in advance, reducing the computational complexity to $\mathcal{O}(|E|)$ and thus offering significant speedup. See Fig. 4 for a visual explanation.

We can consider various placements for the Q , including Q^{circle} [11]. In this study, we adopt a hexagonal lattice Q^{hex} [23, 27] defined by Eq. (4). When minimizing the objective function that arises from the attractive energy f^a , it is advantageous for the points to cluster as closely as possible. In this context, the hexagonal lattice is known for its densest packing structure in space with the least distance ϵ between points and offers computational simplicity. Thus, Q^{hex} is a suitable choice, and we have derived the problem (3).

4.2 Newton Direction for Discrete Optimization

Next, we solve the discrete optimization problem (3). Although this problem is challenging to solve just using simple methods, the coordinate Newton direction of a randomly selected vertex i provides significant insights as mentioned in Sec. 3.4. Therefore, we can offer a high-quality solution to the problem. Let the restricted objective function $f_i^a(x_i)$ be

$$f_i^a(x_i) := \sum_{j \neq i} \frac{w_{i,j} \|x_i - x_j\|^3}{3k}.$$

Its gradient and Hessian matrix are

$$\begin{aligned} \nabla f_i^a(x_i) &= \sum_{j \neq i} \frac{w_{i,j} \|x_i - x_j\|}{k} (x_i - x_j), \\ \nabla^2 f_i^a(x_i) &= \sum_{j \neq i} \frac{w_{i,j} \|x_i - x_j\|}{k} \begin{pmatrix} 1 & 0 \\ 0 & 1 \end{pmatrix} \\ & \quad + \sum_{j \neq i} \frac{w_{i,j}}{k \|x_i - x_j\|} (x_i - x_j)(x_i - x_j)^\top. \end{aligned}$$

This means f_i^a is strictly convex, assuring the Hessian matrix $\nabla^2 f_i^a(x_i)$ is positive definite. This is a large difference from the functions $f(X)$ in the problem (1) and $f^a(X)$ in the problem (3), which are non-convex.

The ordinary updated rule with the coordinate Newton direction is

$$x_i^{\text{new}} \leftarrow x_i - \nabla^2 f_i^a(x_i)^{-1} \nabla f_i^a(x_i).$$

x_i^{new} may not be in the hexagonal lattice Q^{hex} in the problem (3). Thus, we project this x_i^{new} onto the nearest point

in Q^{hex} . We also empirically found that adding a random noise vector to the Newton direction is effective for the optimization process, a strategy similar to the SA in Sec. 3.2. This randomness can help to escape from local minima and to explore the solution space more effectively. In conclusion, the updated rule for the vertex i is

$$x_i^{\text{new}} \leftarrow \text{round}(x_i - \nabla^2 f_i^a(x_i)^{-1} \nabla f_i^a(x_i) + t \cdot r),$$

where $\text{round}(\hat{x})$ denotes the operation assigning \hat{x} to the nearest point in the hexagonal lattice Q^{hex} , r is a random vector with a unit norm, and t is a randomness controlling parameter decreases to zero.

If there is a vertex j such that $x_j = x_i^{\text{new}}$, we swap the positions x_i and x_j to satisfy the condition $x_i \neq x_j$. Otherwise, we just update x_i to x_i^{new} . Refer to Fig. 5 for a visual explanation. Repeating this procedure yields an approximate solution to the problem (3).

4.3 Optimal Scaling

The obtained solution could be too small or too large since we did not care about the scale ϵ . Thus, as the final step, we rescale the placement to improve it.

Let us formulate the optimization problem for the scaling factor $s > 0$. For an initial placement $X = (x_1, \dots, x_n)$, we scale it as $x_i \leftarrow s x_i$ for all i . The problem of minimizing $f(X)$ through scaling is equivalent to minimizing $\phi(s)$ defined by

$$\begin{aligned} \phi(s) &:= \sum_{\{i,j\} \in E} \frac{w_{i,j}(s\|x_i - x_j\|)^3}{3k} - k^2 \sum_{i < j} \log(s\|x_i - x_j\|), \\ \phi'(s) &= \sum_{\{i,j\} \in E} \frac{w_{i,j}\|x_i - x_j\|^3}{k} s^2 - \frac{k^2 n(n-1)}{2s}. \end{aligned}$$

The function $\phi(s)$ is convex, and the optimal scaling factor s^* satisfies $\phi'(s^*) = 0$, which yields

$$s^* = \left(\frac{k^3 n(n-1)}{2 \sum_{\{i,j\} \in E} w_{i,j} \|x_i - x_j\|^3} \right)^{1/3}. \quad (5)$$

This value can be computed in $\mathcal{O}(|E|)$ complexity, enabling us to obtain a better initial placement for the problem (1).

Notably, the optimal solution to the problem (3) is invariant under scaling. Thus, we do not have to care about the scale factor for the hexagonal lattice Q^{hex} as far as we scale the obtained placement by s^* .

4.4 Alternative Approach

To end this section, we explain an alternative approach to the problem (3). We can also solve the problem by updating all vertices simultaneously, not one by one. It means moving all the points $\{x_i\}_{i \in V}$ to arbitrary positions and then assigning all these $|V|$ points to the nearest points on Q^{hex} . The optimal assignment for $\{x_i\}_{i \in V}$ to Q^{hex} is computable by a Hungarian algorithm in $\mathcal{O}(|V|^3)$ time or some heuristic.

They offer advantages such as simplified implementation or avoiding random access to arrays.

Algorithm 1: Proposed algorithm for the initial placement

Input: Graph $G = (V, E)$, Weight $(w_{i,j})_{\{i,j\} \in E}$, Parameters $N_{\text{iter}}^{\text{CN}} \in \mathbb{N}$, and $t_0 > 0$

Output: Initial placement $X = (x_1, \dots, x_n)$

```

1  $t \leftarrow t_0$ ;
2 Sample  $x_i \in Q^{\text{hex}}$  for all  $i \in V$  without replacement;
3 for  $m \leftarrow 0$  to  $N_{\text{iter}}^{\text{CN}}$  do
4   | Select vertex  $i \in V$  randomly;
5   | Draw  $r \in \mathbb{R}^2$  randomly from a unit circle;
6   |  $x_i^{\text{new}} \leftarrow \text{round}(x_i - \nabla^2 f_i(x_i)^{-1} \nabla f_i(x_i) + t \cdot r)$ ;
7   | if  $\exists j \in V$  such that  $x_j = x_i^{\text{new}}$  then
8   |   |  $x_j \leftarrow x_i$ ;
9   |   |  $x_i \leftarrow x_i^{\text{new}}$ ;
10  |   |  $t \leftarrow t - t_0/N_{\text{iter}}^{\text{CN}}$ ;
11  $x_i \leftarrow s^* x_i$  for all  $i \in V$  with  $s^*$  given by Eq. (5);
12 return  $X$ 

```

5 NUMERICAL EXPERIMENT

In this section, we evaluate the proposed algorithm with various numerical experiments. We also confirm that, as stated in Sec. 1, the proposed algorithm efficiently provides a good initial placement even for larger weighted graphs.

5.1 Experimental Setup

We conducted all numerical experiments in this section using C++17 compiled by GCC 10.5.0 on a laptop computer powered by Intel(R) Core(TM) i7-10510U CPU with 16 GB RAM.

For a fair comparison, we implemented the FR algorithm in C++ based on NetworkX version 3.3 [14], SciPy 1.14.1 [32], and utilized the C++ L-BFGS [26, 28] library for the L-BFGS algorithm. We also referred to open-source code of the hexagonal grid [27] and Graphviz version 2.43.0 [7].

We used the 3×2 algorithms. As an initial placement, we used

- random initialization (no prefix),
- the SA initialization obtained by Simulated Annealing (SA-) [11],
- the proposed initialization obtained with coordinate Newton direction (CN-).

As an algorithm to solve the problem (1), we used

- FR algorithm (FR),
- L-BFGS algorithm (L-BFGS).

As parameters, we used initial temperature $t_0 = 1.5$ and the number of iterations $N_{\text{iter}}^{\text{CN}} = 2|V|^3/|E|$ for Algorithm 1, and we also set the total number of iterations of Simulated Annealing (SA) in Sec. 3.2 to the same value. Since the Algorithm 1 requires a computational time proportional to the degree of the selected vertex in each iteration, the expected computational time per iteration is $\mathcal{O}(|E|/|V|)$. Consequently, we can roughly estimate that the total computational time of the proposed algorithm is $\mathcal{O}(|V|^2)$, equivalent to a few iterations of the FR or L-BFGS algorithms. All the codes are available at GitHub [16].

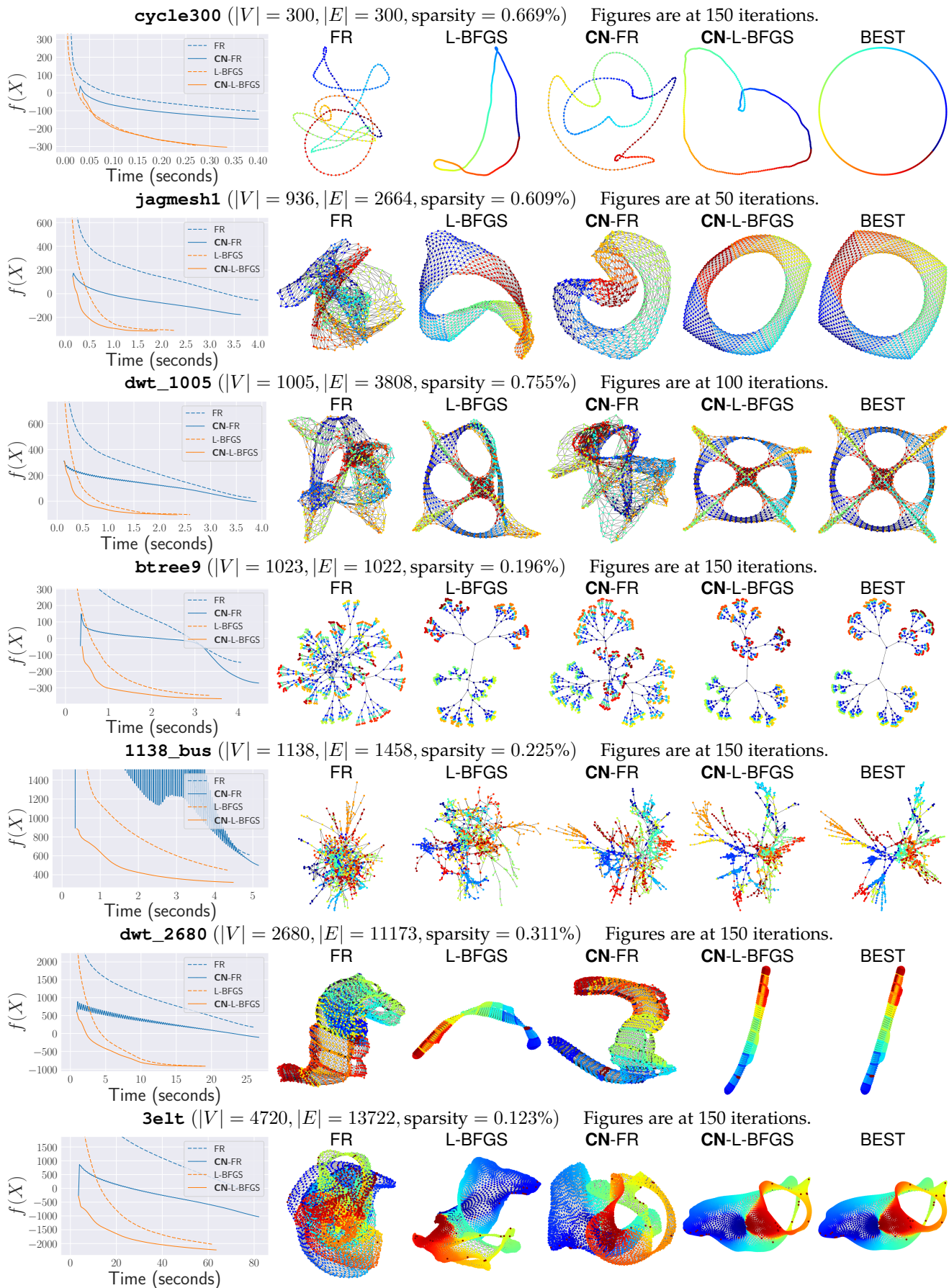


Fig. 6. Experiment results for various graphs. CN denotes Coordinate Newton, representing our proposed methods. See Sec. 5.2 for further details.

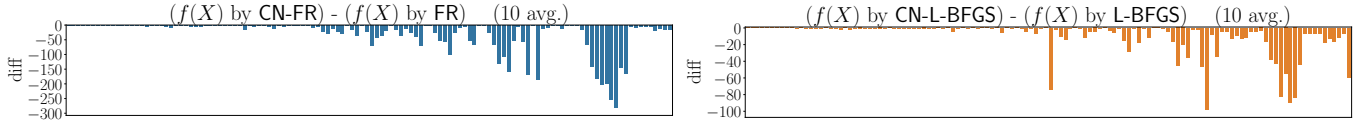


Fig. 7. Comparison of the proposed initialization (CN) with random initialization (no prefix). In almost all cases, the difference is negative, meaning the proposed algorithm performed faster and better than random initialization.

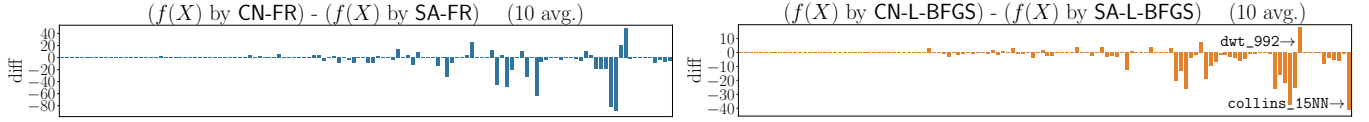


Fig. 8. Comparison of the proposed initialization (CN) with SA initialization (SA) in Ref. [11]. In most cases, the proposed algorithm performed better than the SA initialization.

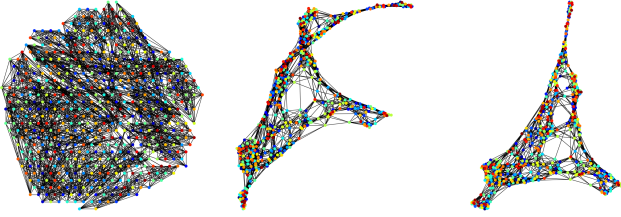


Fig. 9. Spectro_10NN, where the proposed algorithm performed worse than random initialization. Left: Initial placement by CN. Middle and Right: 50th and 200th iteration of CN-L-BFGS.

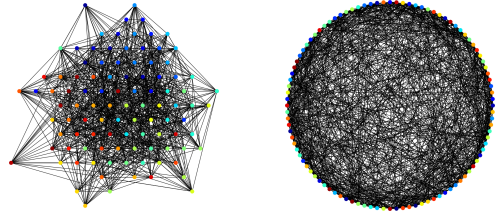


Fig. 10. An example of a case where $w_{i,j} \notin \{0, 1\}$. Left: the result of CN, which is better as the vertices are separated by colors. Right: the result of SA, which is worse as there is no separation.

5.2 Plots and Visualizations

We first show the plots and visualizations of the algorithms in Fig. 6. The experiment details are as follows. We fixed the maximum number of iterations of the FR and L-BFGS algorithms as $N_{\text{iter}}^{\text{FR}} = N_{\text{iter}}^{\text{L-BFGS}} = 200$. We tested with 7 graphs: cycle300, jagmesh1, dwt_1005, btree9, 1138_bus, dwt_2680, and 3elt. Here cycle300 is a cycle graph with 300 vertices, and btree9 is a perfect binary tree with $2^{9+1} - 1 = 1023$ vertices. Other graphs are from Sparse Matrix Collection [5], and these choices are based on Ref. [33].

In Fig. 6, the plots on the left illustrate the objective function values $f(X)$, the average of the ten trials for each algorithm. The graphs on the right are at the iteration in which the most significant difference appeared among $\{50, 100, 150\}$ -th iterations (or at the last iteration if it ended earlier), using seed 1. We obtained the “BEST” column by running at most 500 iterations of CN-L-BFGS. The vertices in the graphs are colored according to vertex indices.

The observations and implications of Fig. 6 are as follows. First, the plots with solid lines for CN generally demonstrate superior performance to those with dashed lines for non-CNese results validate the efficacy of the proposed method. Secondly, the result for 1138_bus exhibits oscillations in the plot, likely due to excessive stepsize leading to overshooting. Adjusting the stepsize could stabilize the proposed method, but we did not modify it to maintain the fairness of the comparisons. The initial values of $f(X)$ with CN-FR are significantly smaller than that with FR, suggesting that the proposed method provides a good initial placement. Thirdly, the visualization results also support the effectiveness of the proposed initial placement. In most cases, placements obtained with CN better reflect the nearly optimal arrangement shown in the “BEST”.

As a side note, regardless of CN or non-CN, the algorithms with L-BFGS consistently outperform those with FR. This finding is consistent with prior research [17]. Regrettably, however, L-BFGS is not yet widely popular in graph drawing. One of the aims of this paper is to the use of L-BFGS in graph drawing, and these results provide solid evidence for the effectiveness of L-BFGS.

5.3 Comparison with Other Initializations

Next, we conducted experiments to evaluate the performance of the proposed algorithm (CN) compared to random initialization (no prefix) and SA initialization (SA) with various graphs.

We used all undirected, connected, non-negative weighted graphs with 1,000 or fewer vertices, which can be generated using the matrices from the Sparse Matrix Collection [5] as adjacency matrices. For fairness, when we compare with SA, we converted the graphs to an unweighted one. It means that we set weights $w_{i,j}$ to 1 if $w_{i,j} > 0$; otherwise, we set it to 0.

For the algorithms with random initial placement, we set $N_{\text{iter}}^{\text{FR}} = N_{\text{iter}}^{\text{L-BFGS}} = 50$, the same as the default parameter in NetworkX [14]. For the CN algorithms, we set $N_{\text{iter}}^{\text{FR}} = N_{\text{iter}}^{\text{L-BFGS}} = 45$, since the pre-processing step is expected to take as long as a few iterations of FR or L-BFGS, as mentioned in Sec. 5.1.

The results are shown in Figs. 7 and 8. The proposed algorithm performed better than random or SA initialization, except for a few cases. As for random initialization, one of such bad cases is Spectro_10NN shown in Fig. 9. The proposed algorithm failed to resolve the twist in the initial placement, shown in the figure, leading to a worse result. Still, the average performance of ten seeds for Spectro_10NN was almost the same as that of

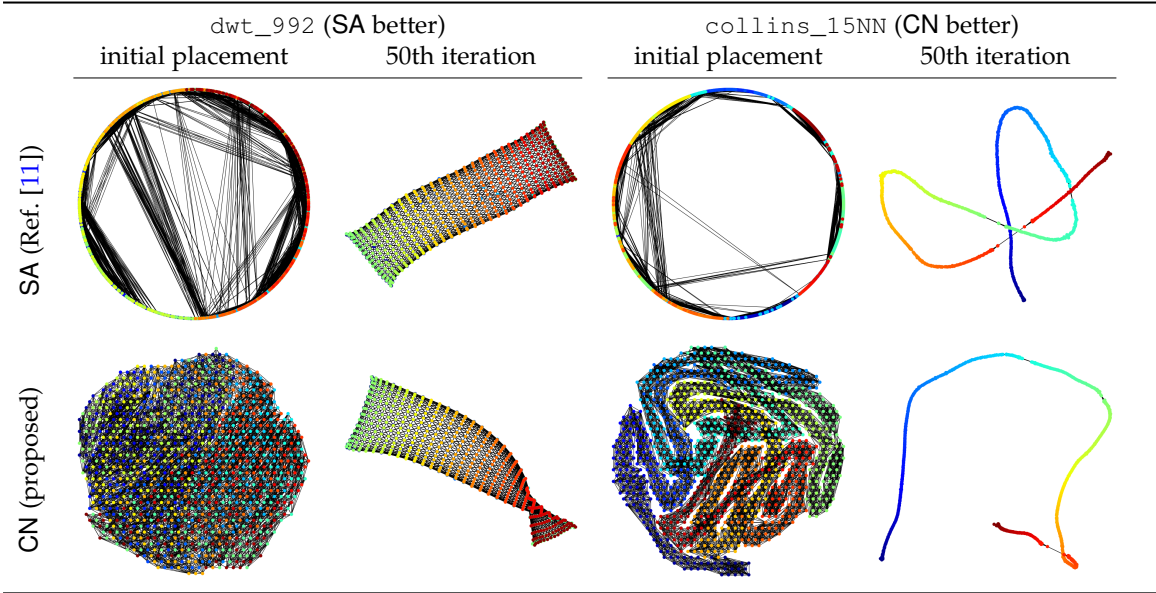


Fig. 11. Visualization results showing initial and 50th iteration placements for `dwt_992` and `collins_15NN`.

the random initialization. Fig. 11 provides examples for comparison with SA initialization. The proposed algorithm outperformed in `collins_15NN` and underperformed in `dwt_992`.

The interpretation of the results is as follows. First, results in Figs. 7 and 8 strongly support the effectiveness of the proposed algorithm. It successfully untangles the twists, leading to better outcomes with faster convergence. Even when the proposed algorithm performed worse, the difference was insignificant in almost all cases. Secondly, the structural difference between the initial placement and the optimal placement potentially affects the convergence speed. For example, the optimal shape of `collins_15NN` is linear, differing from a circle, resulting in SA's performance being inferior to the proposed algorithm, whereas the opposite holds for `dwt_992`. Although the proposed method utilizes a hexagonal lattice Q^{hex} , alternatives such as Q^{circle} may lead to improved performance of the proposed method in some cases.

Furthermore, although this is a case not considered in Ref. [11], we also conducted experiments with CN and SA for a case where the edge weight $w_{i,j}$ is not necessarily in $\{0, 1\}$. We generated a weighted graph with 100 vertices in three groups and 1000 edges randomly, and if the two vertices were in the same group, we set the edge weight to 1.0; otherwise, we set it to 0.1. It exhibits both strong and weak connections. Fig. 10 shows the difference between the two initializations. When we ignore the edge weights and just solve the problem (2), the graph is just an Erdős–Rényi graph, and thus SA cannot find any meaningful structure in the initial placement. In contrast, the proposed algorithm can find the graph's structure, and we can observe that the left graph in Fig. 10 is separated by the groups, i.e., the node color. This result suggests that our proposed algorithm is effective even for weighted graphs, extending the applicability of the pre-processing step.

6 RATIONALE FOR PROPOSED ALGORITHM

This section explains why we took a roundabout approach to solve the problem (1). As we have explained, we first transformed it into the discrete optimization problem (3) and then optimized it using the coordinate Newton direction. Instead, we can naturally consider directly applying the coordinate Newton direction to optimize the problem (1). Is it still effective? We consider the answer is no, and in this section, we explain the reasons behind this conclusion and the rationale for our approach.

6.1 Possible Approach with Coordinate Newton Direction

We first explain a possible approach using the coordinate Newton direction to solve the problem (1). As mentioned in Sec. 3.4, our approach is based on the stochastic coordinate descent and also resembles the Randomized Subspace Newton, one of the subspace methods [2, 9, 12, 15, 25].

Let $f_i: \mathbb{R}^2 \rightarrow \mathbb{R}$ denote the energy function for the vertex i at x_i , defined by

$$f_i(x_i) := \sum_{j \neq i} E_{i,j}(\|x_i - x_j\|). \quad (6)$$

Its gradient, the sum of forces acting on the vertex i , and its Hessian are

$$\begin{aligned} \nabla f_i(x_i) &= \sum_{j \neq i} \left(\frac{w_{i,j} \|x_i - x_j\|}{k} - \frac{k^2}{\|x_i - x_j\|^2} \right) (x_i - x_j), \\ \nabla^2 f_i(x_i) &= \sum_{j \neq i} \left(\frac{w_{i,j} \|x_i - x_j\|}{k} - \frac{k^2}{\|x_i - x_j\|^2} \right) \begin{pmatrix} 1 & 0 \\ 0 & 1 \end{pmatrix} + \\ &\quad \sum_{j \neq i} \left(\frac{w_{i,j}}{k \|x_i - x_j\|} + \frac{2k^2}{\|x_i - x_j\|^4} \right) (x_i - x_j)(x_i - x_j)^\top. \end{aligned}$$

The direct application of stochastic coordinate descent to the problem (1) is as follows. We randomly select a vertex i and apply Newton's method or its regularized variant to f_i

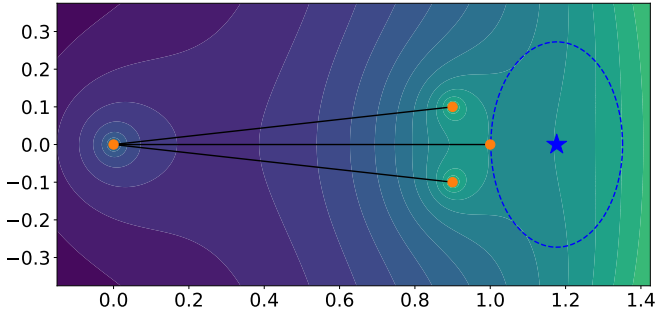


Fig. 12. The inaccurate quadratic approximation. The blue star indicates the optimal solution for the quadratic approximation of $f_1(x_1)$, but this differs significantly from the situation shown by the contour lines.

using the gradient and Hessian. Then, we update the position of vertex i and repeat this process until convergence. We do not go through any discrete optimization problem with this approach. Then, this approach fails to work effectively in practice. In the following, we explain the reasons behind this failure with non-trivial examples.

6.2 Inaccuracy of Quadratic Approximation

One of the reasons why it fails is the inaccuracy of quadratic approximation; particularly, a specific issue arises when we restrict the optimization to a coordinate block.

Let G be a graph with $V = \{1, 2, 3, 4\}$ and $E = \{\{1, 2\}, \{2, 3\}, \{2, 4\}\}$. Set $k = 1/2$ and assign all positive edge weights $w_{i,j} = 1$ for every edge in E . The position of the vertices are

$$X = \begin{pmatrix} 1 & 0 & 0.9 & 0.9 \\ 0 & 0 & +0.1 & -0.1 \end{pmatrix}.$$

We show the contour of $f_1(x_1)$ in Fig. 12.

The key point of this example is that the Hessian

$$\nabla^2 f_1(x_1) = \begin{pmatrix} 4.25 & 0 \\ 0 & 1.75 \end{pmatrix}$$

is positive definite and well-conditioned. Despite this favorable property of the Hessian, the coordinate Newton direction for x_1 results in a deviation from the global optimum. This issue arises from the inaccurate approximation of f_1 in the restricted block coordinates x_1 . The attractive force from vertex 2 and the repulsive forces from vertices 3 and 4 cancel each other out, leading to a highly inaccurate quadratic approximation. This deficiency cannot be entirely resolved by modifying Newton's method, as it is an intrinsic and unavoidable limitation of the stochastic coordinate descent.

6.3 Ignorance of Other Vertices' Movements

Another reason is the ignorance of other vertices' movements when optimizing each vertex individually. When optimizing for a vertex i , the coordinate Newton direction treats all other vertices j ($j \neq i$) as fixed.

Fig. 13 illustrates this issue. Consider a subset of vertices forming a mesh-like structure in G , where all vertices receive forces in the directions indicated by the blue arrows. In this situation, the FR and L-BFGS algorithms move all vertices simultaneously, allowing the simulation

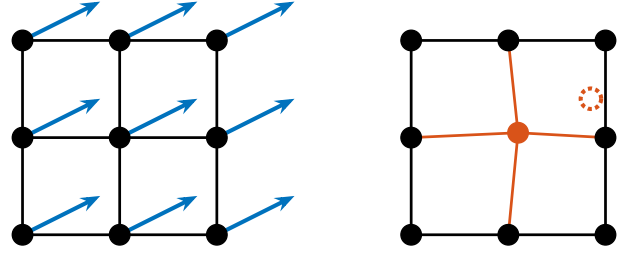


Fig. 13. The ignorance of other vertices' movements. Although the blue arrows show the forces in this situation, the red vertex barely moves by the coordinate Newton direction.

or optimization to proceed without issues. In contrast, the stochastic coordinate descent, as shown on the right side of the figure, brings stagnation. Here, all other vertices are considered fixed. Thus, optimizing the red vertex results in minimal movement, as its directly connected neighbors impede it. As a result, even after numerous iterations, little optimization is achieved. Thus, ignoring the other vertices' movements can be a significant limitation of the coordinate Newton method.

6.4 Rationale for Proposed Method

As discussed in Secs. 6.2 and 6.3, directly applying the coordinate Newton direction to f_i does not work effectively. Our proposed method resolves these issues by transforming the problem (1) into the problem (3) in Sec. 4.1, and optimizing f_i^a on Q^{hex} .

Regarding the issue in Sec. 6.2, this transformation brings the convexity of the problem, making the quadratic approximation more accurate than the original problem. Regarding the issue in Sec. 6.3, the discrete point set Q ensures that the stepsize is larger than ϵ , as each point is always separated by at least ϵ . This large stepsize prevents stagnation in the optimization and helps explore the solution space more efficiently. Furthermore, this transformation also brings the benefit of reducing computational complexity from $\mathcal{O}(|V|^2)$ to $\mathcal{O}(|E|)$.

Thus, converting the problem is crucial to provide a high-quality initial placement with the coordinate Newton direction. There may also be better transformation methods, and further exploration is warranted.

7 DISCUSSION

In this section, we discuss the future directions of this research. Firstly, we discuss combining our algorithm with conventional techniques, such as the multilevel approach. Secondly, we explore the applications beyond the scope of graph drawing. Finally, we conclude this paper.

7.1 Combination with Other Techniques

This paper has demonstrated the effectiveness of the proposed method on various graphs, and it might also be applicable to larger-scale problems. In general, approximating or simplifying the model itself is one strategy for dealing with large graphs. Examples of such approaches include employing stress majorization [10], the n -body simulation using

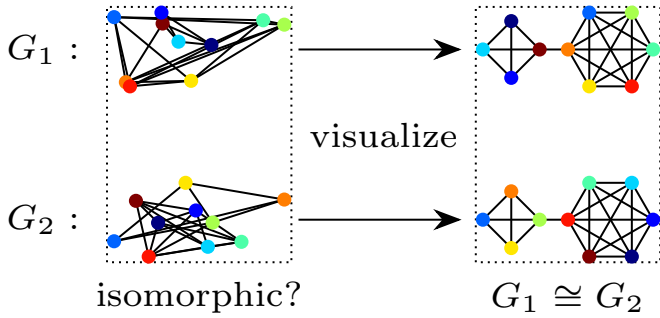


Fig. 14. Illustration of the relationship between graph drawing and graph isomorphism. If we can draw graphs G_1 and G_2 symmetrically, then it is clear that $G_1 \cong G_2$.

multipole expansions [13], approximating by the Barnes–Hut approximation [1], and gradually refining the layouts using a multilevel approach [18]. For instance, the Scalable Force-Directed Placement (sfdp) of Graphviz [7] proposed in Ref. [18] employs a multilevel approach to accelerate processing for larger graphs by progressively coarsening vertices.

In particular, the coarsening operation in sfdp does not critically conflict with the proposed method, making it feasible to combine both approaches. Specifically, by iteratively applying the proposed method to the entire coarsened graph or groups of vertices consolidated through coarsening, it is possible to extend its applicability to larger-scale problems. We can expect this approach to yield faster and higher-quality solutions. Addressing this integration is one of the challenges for future research.

In addition, the FR force model is sometimes used not only in \mathbb{R}^2 but also in \mathbb{R}^3 [22]. Although we have to modify some parts of the proposed algorithm for \mathbb{R}^3 , such as the hexagonal lattice, its application would be easy.

7.2 Application to Other Problems

In this subsection, we briefly discuss and explore the potential applicability of stochastic coordinate descent to a broader range of problems. Although we utilized the coordinate Newton direction only for the optimization problem (1), we can see that its application is not necessarily limited to the FR force model alone.

In general, the optimization problem (1) is more broadly treated as “objective functions arising from graphs” [29]:

$$\underset{X \in \mathbb{R}^{2 \times n}}{\text{minimize}} \quad f(X) = \sum_{\{i,j\} \in E} f_{i,j}(x_i, x_j) + \lambda \sum_{i=1}^n \Omega_i(x_i),$$

where Ω_i is a regularization term for vertex i and $\lambda > 0$ is a regularization parameter. The optimization problem (1) is a special case of this problem class. The authors of Ref. [29] claim that coordinate descent, only with coordinate gradients, effectively solves such problems. A variant of the proposed method utilizing the coordinate Newton direction can also be effective for such problems.

For instance, the graph isomorphism problem is a possible application. The graph isomorphism problem is a well-known combinatorial optimization problem to determine whether two graphs, G_1 and G_2 , are isomorphic, i.e.,

Algorithm 2: Fruchterman–Reingold algorithm

Input: Graph $G = (V, E)$, Weights $(w_{i,j})_{\{i,j\} \in E}$,
Parameters $N_{\text{iter}}^{\text{FR}} \in \mathbb{N}$, $t_0 > 0$, and
Initial placement $X = (x_1, \dots, x_n)$

Output: Final placement X

```

1  $t \leftarrow t_0$ ;
2 for  $m \leftarrow 1$  to  $N_{\text{iter}}^{\text{FR}}$  do
3   compute gradient  $\nabla f_i(x_i)$  for all  $i \in V$ ;
4    $x_i^{\text{new}} \leftarrow x_i - t \frac{\nabla f_i(x_i)}{\|\nabla f_i(x_i)\|}$  for all  $i \in V$ ;
5    $x_i \leftarrow x_i^{\text{new}}$ ;
6    $t \leftarrow t - t_0/N_{\text{iter}}^{\text{FR}}$ ;
7   if convergence condition is satisfied then
8     break;
9 return  $X$ ;

```

$G_1 \cong G_2$. The graph isomorphism problem is closely related to the graph drawing. Drawing a graph in a way that reveals its symmetry is at least as difficult as the graph isomorphism problem [6]. Indeed, if we can draw two graphs G_1 and G_2 in the same way, it becomes evident that $G_1 \cong G_2$. See Fig. 14 for reference. When we relax it to a continuous optimization problem on Riemannian manifolds [20], we might be able to apply the stochastic coordinate descent or coordinate Newton direction to this problem as well. Investigating the variant of our proposed algorithm for these problems constitutes one of the future research directions.

7.3 Conclusion

In this study, we proposed a new initial placement with the coordinate Newton direction for the FR force model. The obtained initial placements have fewer twists than the random initialization, leading to faster convergence and better visualization. Numerical experiments revealed that the proposed method is effective across various graphs, extending the applicability of the pre-processing step. We expect that the proposed method may advance the graph drawing of the FR force model. We also hope it highlights the potential of the stochastic coordinate descent and its variants for addressing a broader range of graph-related optimization problems.

8 SUPPLEMENTARY INFORMATION

As supplementary information, this section explains how to solve the problem (1) and obtain the final placement for the graph drawing.

8.1 Fruchterman–Reingold Algorithm

The Fruchterman–Reingold algorithm [8] is the original force-directed algorithm and the most standard approach for the FR force model. The pseudo-code of the FR algorithm is shown in Algorithm 2, which can be regarded as a variant of gradient (steepest) descent method with the function f_i in Eq. (6) [30].

The Algorithm 2 is based on the original code [8] and implementation in NetworkX [14] with some omitted details. The initial placement X is often drawn from a uniform

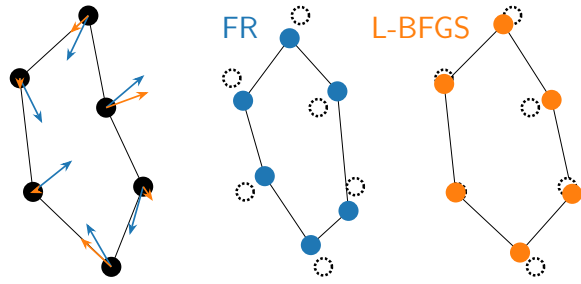


Fig. 15. Comparison of the FR algorithm and the L-BFGS algorithm. While the FR algorithm updates vertices in a descent direction with a fixed stepsize (blue arrows), the L-BFGS algorithm adjusts them differently since it utilizes approximated inverse Hessian (orange arrows).

distribution on a unit square. The parameter t denotes the temperature, which governs the stepsize along the steepest descent. As the temperature gradually decreases, the algorithm converges to a particular placement, though this placement is not necessarily the local optimum to the problem (1).

8.2 L-BFGS Algorithm

Another approach to solving the optimization problem (1) is to use the Limited-memory Broyden–Fletcher–Goldfarb–Shanno (L-BFGS) algorithm [17]. Using only a few recent gradient vectors, the L-BFGS algorithm approximates the inverse Hessian of the objective function f [24]. L-BFGS is known to be very efficient for large-scale optimization problems, and the superior performance of the L-BFGS algorithm to the FR algorithm reported in Ref. [17] also indicates this fact. Refer to Fig. 15 for a comparison to the FR algorithm.

For the optimization problem (1), we can apply the L-BFGS algorithm via flattening the matrix $X \in \mathbb{R}^{2 \times n}$ to a vector $\bar{X} \in \mathbb{R}^{2n}$. It is worth noting that this method ignores the structure of X and treats it just as a general optimization problem. Therefore, there is room for improvement by explicitly leveraging the graph structure, which our proposed method accomplished.

9 ACKNOWLEDGMENT

The author would like to express our sincere gratitude to PL Poirion and Andi Han for their insightful discussions, which have greatly inspired and influenced this research.

The author also thanks the developers of NetworkX and Graphviz. Their excellent work has been a great help in conducting this research.

This work was partially supported by JSPS KAKENHI (23H03351, 24K23853) and JST ERATO (JPMJER1903).

REFERENCES

[1] J. Barnes and P. Hut, “A hierarchical $O(N \log N)$ force-calculation algorithm,” *Nature*, vol. 324, no. 6096, pp. 446–449, 1986. [Online]. Available: <https://www.nature.com/articles/324446a0>

[2] C. Cartis, J. Fowkes, and Z. Shao, “Randomised subspace methods for non-convex optimization, with

applications to nonlinear least-squares,” 2022. [Online]. Available: <http://arxiv.org/abs/2211.09873>

[3] S.-H. Cheong and Y.-W. Si, “Snapshot Visualization of Complex Graphs with Force-Directed Algorithms,” in *2018 IEEE International Conference on Big Knowledge (ICBK)*, 2018, pp. 139–145. [Online]. Available: <https://ieeexplore.ieee.org/document/8588785/?arnumber=8588785>

[4] G. Csardi and T. Nepusz, “The igraph software package for complex network research,” *InterJournal*, vol. Complex Systems, p. 1695, 2006. [Online]. Available: <https://igraph.org>

[5] T. A. Davis and Y. Hu, “The University of Florida sparse matrix collection,” *ACM Transactions on Mathematical Software (TOMS)*, vol. 38, no. 1, pp. 1–25, 2011.

[6] P. Eades, “A heuristic for graph drawing,” *Congressus numerantium*, vol. 42, no. 11, pp. 149–160, 1984.

[7] J. Ellson, E. Gansner, L. Koutsofios, S. C. North, and G. Woodhull, “Graphviz—Open Source Graph Drawing Tools,” in *Graph Drawing*, P. Mutzel, M. Jünger, and S. Leipert, Eds. Springer, 2002, pp. 483–484.

[8] T. M. J. Fruchterman and E. M. Reingold, “Graph drawing by force-directed placement,” *Software: Practice and Experience*, vol. 21, no. 11, pp. 1129–1164, 1991. [Online]. Available: <https://onlinelibrary.wiley.com/doi/abs/10.1002/spe.4380211102>

[9] T. Fuji, P.-L. Poirion, and A. Takeda, “Randomized subspace regularized Newton method for unconstrained non-convex optimization,” 2022. [Online]. Available: <http://arxiv.org/abs/2209.04170>

[10] E. R. Gansner, Y. Koren, and S. North, “Graph Drawing by Stress Majorization,” in *Graph Drawing*, D. Hutchison *et al.*, Eds. Springer Berlin Heidelberg, 2005, vol. 3383, pp. 239–250. [Online]. Available: http://link.springer.com/10.1007/978-3-540-31843-9_25

[11] F. Ghassemi Toosi, N. S. Nikolov, and M. Eaton, “Simulated Annealing as a Pre-Processing Step for Force-Directed Graph Drawing,” in *Proceedings of the 2016 on Genetic and Evolutionary Computation Conference Companion*, ser. GECCO ’16 Companion. Association for Computing Machinery, 2016, pp. 997–1000. [Online]. Available: <https://dl.acm.org/doi/10.1145/2908961.2931660>

[12] R. Gower, D. Kovalev, F. Lieder, and P. Richtarik, “RSN: Randomized subspace newton,” in *Advances in Neural Information Processing Systems*, H. Wallach, H. Larochelle, A. Beygelzimer, F. dAlché-Buc, E. Fox, and R. Garnett, Eds., vol. 32. Curran Associates, Inc., 2019. [Online]. Available: https://proceedings.neurips.cc/paper_files/paper/2019/file/bc6dc48b743dc5d013b1abaebd2faed2-Paper.pdf

[13] L. Greengard and V. Rokhlin, “A fast algorithm for particle simulations,” *Journal of Computational Physics*, vol. 73, no. 2, pp. 325–348, 1987. [Online]. Available: <https://www.sciencedirect.com/science/article/pii/0021999187901409>

[14] A. Hagberg, P. J. Swart, and D. A. Schult, “Exploring network structure, dynamics, and function using NetworkX,” Los Alamos National Laboratory (LANL), Los Alamos, NM (United States), Tech. Rep., 2008.

[15] R. Higuchi, P.-L. Poirion, and A. Takeda, “Fast

- Convergence to Second-Order Stationary Point through Random Subspace Optimization,” 2024. [Online]. Available: <http://arxiv.org/abs/2406.14337>
- [16] H. Hiroki, “Hari64boli64/Initial Placement for Fruchterman–Reingold Force Model with Coordinate Newton Direction.” [Online]. Available: https://github.com/hari64boli64/Initial_Placement_for_Fruchterman-Reingold_Force_Model_with_Coordinate_Newton_Direction
- [17] H. Hosobe, “Numerical optimization-based graph drawing revisited,” in *2012 IEEE Pacific Visualization Symposium*, 2012, pp. 81–88.
- [18] Y. Hu, “Efficient, high-quality force-directed graph drawing,” *The Mathematica journal*, vol. 10, pp. 37–71, 2006. [Online]. Available: <https://api.semanticscholar.org/CorpusID:14599587>
- [19] T. Kamada and S. Kawai, “An algorithm for drawing general undirected graphs,” *Information Processing Letters*, vol. 31, no. 1, pp. 7–15, 1989. [Online]. Available: <https://www.sciencedirect.com/science/article/pii/0020019089901026>
- [20] S. Klus and P. Gelß, “Continuous optimization methods for the graph isomorphism problem,” 2023. [Online]. Available: <http://arxiv.org/abs/2311.16912>
- [21] S. G. Kobourov, “Spring Embedders and Force Directed Graph Drawing Algorithms,” 2012. [Online]. Available: <http://arxiv.org/abs/1201.3011>
- [22] G. Kortemeyer, “Virtual-Reality graph visualization based on Fruchterman-Reingold using Unity and SteamVR,” *Information Visualization*, vol. 21, no. 2, pp. 143–152, 2022. [Online]. Available: <https://doi.org/10.1177/14738716211060306>
- [23] J. Li, Y. Tao, K. Yuan, R. Tang, Z. Hu, W. Yan, and S. Liu, “Fruchterman–reingold hexagon empowered node deployment in wireless sensor network application,” *Sensors*, vol. 22, no. 5179, 2022. [Online]. Available: <https://www.mdpi.com/1424-8220/22/14/5179>
- [24] D. C. Liu and J. Nocedal, “On the limited memory BFGS method for large scale optimization,” *Mathematical Programming*, vol. 45, no. 1, pp. 503–528, 1989. [Online]. Available: <https://doi.org/10.1007/BF01589116>
- [25] R. Nozawa, P.-L. Poirion, and A. Takeda, “Randomized subspace gradient method for constrained optimization,” 2023. [Online]. Available: <http://arxiv.org/abs/2307.03335>
- [26] N. Okazaki, “Chokkan/liblbfgs,” 2024. [Online]. Available: <https://github.com/chokkan/liblbfgs>
- [27] A. J. Patel, “Hexagonal Grids,” Red Blob Games, Tech. Rep., 2013. [Online]. Available: <https://www.redblobgames.com/grids/hexagons/>
- [28] Y. Qiu, “Yixuan/LBFGSpp,” 2024. [Online]. Available: <https://github.com/yixuan/LBFGSpp>
- [29] B. Recht and S. J. Wright, “Optimization for modern data analysis,” 2019. [Online]. Available: https://people.eecs.berkeley.edu/~brecht/opt4ml_book/
- [30] D. Tunkelang, “A numerical optimization approach to general graph drawing,” Ph.D. dissertation, Carnegie Mellon University, 1999.
- [31] T. L. Veldhuizen, “Dynamic Multilevel Graph Visualization,” 2007. [Online]. Available: <http://arxiv.org/abs/0712.1549>
- [32] P. Virtanen *et al.*, “SciPy 1.0: Fundamental algorithms for scientific computing in python,” *Nature Methods*, vol. 17, pp. 261–272, 2020.
- [33] J. X. Zheng, S. Pawar, and D. F. M. Goodman, “Graph Drawing by Stochastic Gradient Descent,” *IEEE Transactions on Visualization and Computer Graphics*, vol. 25, no. 9, pp. 2738–2748, 2019. [Online]. Available: <https://ieeexplore.ieee.org/document/8419285>

Hiroki Hamaguchi Graduate School of Information Science and Technology, The University of Tokyo, Tokyo, Japan.

Naoki Marumo Graduate School of Information Science and Technology, The University of Tokyo, Tokyo, Japan.

Akiko Takeda Graduate School of Information Science and Technology, The University of Tokyo, Tokyo, Japan. Center for Advanced Intelligence Project, RIKEN, Tokyo, Japan.